Photochemical Decoloration of Remazol Brilliant Blue and Uniblue A in the Presence of Fe 3+ and H 2 O 2

ARTICLE *in* ENVIRONMENTAL SCIENCE AND TECHNOLOGY · SEPTEMBER 1999

Impact Factor: 5.33 · DOI: 10.1021/es980995+

4 AUTHORS, INCLUDING:

J. Kiwi
École Polytechnique Fédérale de Lausanne
328 PUBLICATIONS **10,953** CITATIONS
SEE PROFILE

Victor A Nadtochenko
Russian Academy of Sciences
110 PUBLICATIONS **1,559** CITATIONS
SEE PROFILE

Environ. Sci. Technol. **1999**, *33,* 3145−3151

Photochemical Decoloration of Remazol Brilliant Blue and Uniblue A in the Presence of Fe^{3+} and H_2O_2

F. HERRERA,[†] J. KIWI,*[,†] A. LOPEZ,[‡] AND V. NADTOCHENKO*[,†]

Institute of Physical Chemistry, Swiss Federal Institute of Technology (EPFL), 1015 Lausanne, Switzerland and CNR-IRSA, Department of Water Chemistry and Technology, Via F. de Blasio 5, Bari 70123, Italy

The primary fast kinetic steps of the decoloration of the nonbiodegradable textile dyes Remazol Brilliant Blue R and its close analogue, Uniblue A, were studied in the presence of the Fe^{3+}/H_2O_2 under light irradiation. Special attention was devoted to the visible excitation at wavelengths >400 nm during dye decoloration. Stopped-flow experiments under light irradiation were carried out at different wavelengths. Laser flash photolysis suggested that electron transfer between the excited dye and Fe^{3+} is the initiating step, either as a bimolecular process ($D^* + Fe^{3+} \rightarrow D^{\bullet+} + Fe^{2+}$) or through a dye/iron complex ($D^* + Fe^{3+} \rightarrow (D\cdots Fe^{3+}) \rightarrow D^{\bullet+} + Fe^{2+}$). A direct correlation was found between the absorption spectrum of the dye and the rate observed for dye decoloration as a function of the wavelength of light used. The latter rate was kinetically modeled using a radical-chain sequence of reactions, obtaining a good agreement between the modeling and the experimental data. A meaningful acceleration during the initiation step in the radical-chain reaction by Fe^{3+}/H_2O_2 is observed involving the photochemical reduction of Fe(III) to Fe(II). The photodissociation reaction of the $[D\cdots Fe^{3+}]$ complex is seen to be more important in the initiation of the chain reaction than the bimolecular quenching between D^* and Fe^{3+}. The latter observation is also related to the enhancement of the decoloration rate observed under light irradiation. The usefulness of the reactions described above is related to the beneficial effect of the visible light activation of the decoloration of nonbiodegradable reactive textile dyes by Advanced Oxidation Technologies (AOTs).

Introduction

Advanced Oxidation Technologies are mainly based on oxidative reactions by $HO^\bullet$ radicals generated by various methods such as O_3/UV, H_2O_2/UV, O_3/H_2O_2/UV photolysis, TiO_2 photocatalysis, and photoassisted Fe^{3+}/H_2O_2 processes (*1*). This last method has gained in importance during the last few years (*2*) as it is considered a promising process for the decontamination of waste waters. This study focuses in the decoloration of two reactive dyes Remazol Brilliant Blue R (RBB) and Uniblue A (UB) via AOTs processes. The textile dye RBB contains the alkyl sulfonate anchor group ("bridge") enabling effective binding to the fiber.

RBB is not a biodegradable dye and is manufactured with other Remazol reactive dyes by Hoechst Portugesa S.A. Aqua-Ambiente, Portugal. Amino-anthraquinone dyes have the same chromophore groups as RBB and UB. Concentrations >40 ppm of RBB and other Remazol reactive dyes have been observed in washwaters of textile manufacturing sites in Southern Europe and end up in waste streams. This occurs in spite of the treatment plants built during the last 30 years. These facilities to treat residual dyes have not been able to increase the transparency of streams and lakes in parts of Southern Europe. The problem remains in meeting the effluent color standards. Traditional technologies, such as activated C-adsorption, chemical coagulation, and reverse osmosis, have been used to treat textile waste waters but they transfer the contaminant from the waste water to solid waste. Fast kinetic spectroscopy and stopped-flow of the decoloration of nonbiodegradable reactive textile dyes using Fe^{3+}/H_2O_2 are presented in this study (*2*, *3*).

During recent years, it is recognized that two important reactions, (1a) and (1b), occurring during the degradation of pollutants, are enhanced due to Fe^{3+}/H_2O_2 in photoassisted reactions

$$H_2O_2 + h\nu(\lambda < 320\ \text{nm}) \rightarrow HO^\bullet + HO^\bullet \qquad (1a)$$

$$FeOH^{2+} + h\nu(\lambda < 320\ \text{nm}) \rightarrow Fe^{2+} + HO^\bullet \qquad (1b)$$

Recently, by steady-state photolysis (*2*, *3*) and by time-resolved laser spectroscopy (*4*−*6*), it was shown that in Fe^{3+}/H_2O_2-mediated processes, photolysis of various $Fe(III)X_{aq}^{2+}$ (X = Cl, PhO) complexes takes place. Subsequent processes may involve the anions in solution like Cl^- when HCl or $FeCl_3$ was used as a reagent; $FeCl_{aq}^{2+} \xrightarrow{\lambda < 390\ \text{nm}} Fe^{2+} + Cl^\bullet$ leading to the formation of $Cl_2^{\bullet-}$ ion radical due to $Cl^\bullet + Cl^- \xrightarrow{k_{diff}} Cl_2^{\bullet-}$. Under adequate experimental conditions in the presence of phenol, Fe^{3+} complexes absorbing in the UV-vis have been shown to photodissociate, $FeOPh^{2+} \xrightarrow{h\nu} Fe^{2+} + PhO^\bullet$ (*4*).

An important step during Fe^{3+}/H_2O_2 mediated processes is the photoreduction of Fe(III) to Fe(II) because the reaction of Fe(II) with H_2O_2 leads to $^\bullet OH$ radical formation (*7*). The bimolecular reaction of the $Fe(III)_{aq}$* excited complex with an organic compound (*8*) is not important because the lifetime of $Fe(III)X_{aq}^{2+}$ *(X = $^\bullet OH$, $Cl^\bullet$, $PhO^\bullet$), of 10^{-8} s, is too short to have a meaningful reaction probability during the bimolecular reaction time between $Fe(III)_{aq}$* and the dyes (*4*, *5*). The quantum yield of photodissociation of $Fe(III)X_{aq}^{2+}$ (X = $^\bullet OH$, $Cl^\bullet$) is $\phi = 0.21$ ($^\bullet OH$), $\phi = 0.5$ ($Cl^\bullet$) at $\lambda_{exc} = 347$ nm (*4*). The scientific literature reports that the quantum yield of $Fe(III)OH_{aq}^{2+}$ dissociation increases as λ used decreases (*9*). The absorption of H_2O_2 and $Fe(III)X_{aq}^{2+}$ drastically limits the relevance of these chromophores during visible light photoassisted Fenton processes as addressed in the present study. Degradation of pollutants by adding oxalic acid to Fe^{3+}/H_2O_2 involves the photodissociation of the ferrioxalate complex with an acceleration of the observed degradation kinetics (*10*).

This work intends to present: (1) a study of the most important fast kinetic steps during the decoloration of the reactive dyes RBB and UB in the presence of the Fe^{3+}/H_2O_2 by laser photolysis, (2) the characteristics of the complex formation between the dye and Fe^{3+} observed spectrophotometrically, (3) the quenching of RBB* and UB* by Fe^{3+}, H_2O_2, and O_2 undertaken by laser photolysis to elucidate the

* Corresponding authors: phone: 41+21-693-3621; fax: 41+21-693-4111; e-mail: john.kiwi@dcqm.epfl.ch and victor.nadtochenko@dcqm.epfl.ch.

[†] Swiss Federal Institute of Technology.

[‡] CNR-IRSA, Department of Water Chemistry and Technology.

10.1021/es980995+ CCC: $18.00
Published on Web 08/07/1999

interaction of UB* and RBB* with other solution components during photoassisted Fenton reactions, (4) the mathematical modeling of decoloration kinetics measured by stopped-flow under illumination with the aim of establishing the radical reaction sequence for the most important dark/photochemical steps in agreement with the experimental data.

The aim of this study is to present the kinetic steps observed during the decoloration of Remazol Brilliant Blue on a real time scale as the decoloration progressed. From about 40 ns, the pulse laser duration is ~15 ns and going progressively through the microsecond and millisecond region up to (80 ms) to show the stopped-flow measurements.

Experimental Section

Materials. The H_2O_2, $Fe(ClO_4)_3 \cdot 9H_2O$, and $HClO_4$ were Fluka p.a. and were used as received without further purification. The pH values of the solutions were adjusted to the desired values with $HClO_4$. Remazol Brilliant Blue R (RBB), MW = 626 and λ_{max} = 590 nm, with $\epsilon_{590\ nm}$ = 5820 $(M\ cm)^{-1}$ was industrial grade and a gift from the company mentioned in the Introduction. Uniblue A sodium salt (UB) was Aldrich 29,640-9, p.a. grade, MW = 506.49, λ_{max} = 594 nm, with $\epsilon_{594\ nm}$ = 5570 $(M\ cm)^{-1}$.

Laser Flash Photolysis and Time-Resolved Spectroscopy. Laser photolysis was carried out using the first harmonic (λ = 694 nm) and second harmonic (λ = 347 nm) of a JK-2000 ruby laser operated in the Q-switched mode. The pulse width was about 15 ns and the highest energy per pulse was ~18 mJ (λ = 347 nm). During the studies, the laser pulse energy was monitored and the experimental results were normalized accordingly. The mean area of the laser beam was 0.5 cm^2. The detection of the transient absorption changes was performed via an EGG photomultiplier with a rise time of about 5 ns. A description of the laser system has been previously reported elsewhere (*4*). The beam of Xe-light discharge lamp (450 W, Osram GmbH, Berlin, Germany) was employed to monitor the detection of the intermediates, and the wavelength region of interest was narrowed with Schott SKF pass-band filters. These filters allowed the beam to come through in a region of $\Delta\lambda$ = 20 nm, centered in each case at the wavelength of interest. The decomposition of both dyes was negligible when the Fenton reagent was added immediately before taking the spectra. Experiments were carried out in aerobic and anaerobic conditions in 1 cm silica cells. The anaerobic conditions were obtained by purging the solution for 30 min with Ar gas before each experiment.

Steady-State Photolysis and Stopped-Flow Studies. Stopped-flow experiments were carried out by means of an Applied Photophysics unit, and the sample solution was kept in a 2 mm optical cell. A single beam spectrophotometer was used to follow the optical density variation during the stopped-flow measurements under light irradiation. Steady-state photolysis was carried out by a Xe-450 W discharge lamp. The IR radiation was filtered by water cell (path length = 6 cm). Sample cells were thermostated during irradiation. Narrow band-pass filters and even narrower line-pass filters (Schott Glassworks, W-6500, Mainz, Germany) and interference filters were used to select a spectral range and isolate the bands of interest in the visible and UV spectral regions. The excitation beam is parallel with the one used for detection of the intermediates as a function of time. The difference between the two beams is their use in different spectral regions. The spectral zones [λ_1–λ_2] under study and the wavelength of the detection beam are different and were defined in each case via appropriate filters. The monitoring light beam transmitted through the stopped-flow cell was measured by a silicon photodiode detector head, model 71882, Oriel Corporation, after passing through a Baush and Lomb UV-vis monochromator blazed at 350 nm with a variable slit assembly. During this work, the long wavelength absorbance of each dye RBB or UB at λs around 600 nm were studied. The signals from the photodiode were registered and stored in a Tektronix TDS 640 A4 digitizing oscilloscope for further processing. In this way, it was possible to plot the changes in molar optical absorption (*A*) with of a Power MacIntosh 4400/200 using the program Igor 3.11 and transduce the experimental signals into the required kinetic curves. The light flux was measured with a radiometer model 65A, Yellow Springs Instruments Co., Yellow Springs. Analyses of the absorbance in solution were carried out via an Hewlett Packard 8452 diode array spectrophotometer.

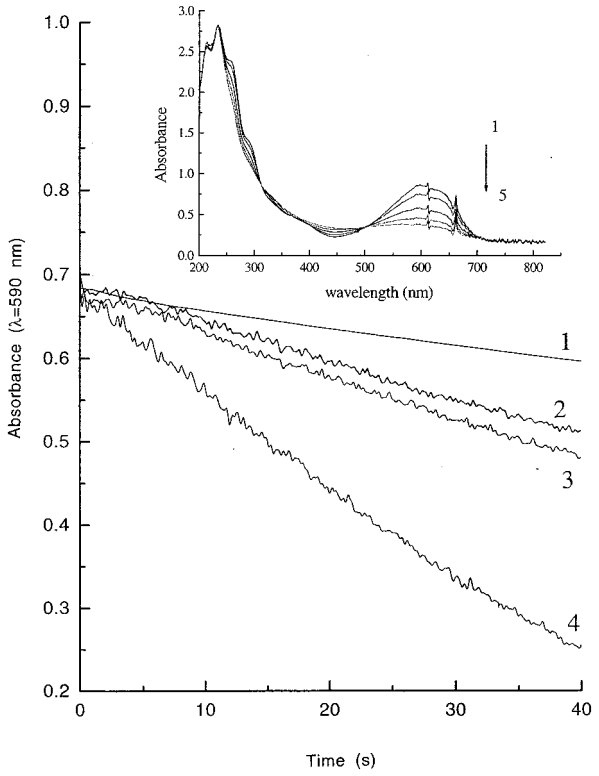

FIGURE 1. Decoloration of Uniblue A mediated by Fe^{3+}/H_2O_2 followed by stopped-flow. [Fe^{3+}] = 0.6 mM; [H_2O_2] = 12.5 mM; [Uniblue A] = 0.1 mM; pH = 2.4. Trace 1 in the dark; trace 2 under light λ > 550 nm (incident light power 0.85 W/cm^2); trace 3 under light λ > 400 nm (incident light power 1.05 W/cm^2); trace 4 under full Xe lamp illumination (incident light power 1.2 W/cm^2); inset, spectral changes of Uniblue A during dark decoloration by Fe^{3+}/H_2O_2. Spectral traces 1–5 taken at times 0, 2, 4, 6, and 8 min after the beginning of the reaction. For other experimental conditions, see text to Figure 1.

Computer Calculations. The software required for modeling the reaction sequence was essentially an ACUCHEM Program in Fortran IV by W. Braun, J. T. Herron, and D. Kahaner from the National Bureau of Standards, Gaithersburg, MD 20899. This program was interconnected with a routine written for MatLab 4.2 platform (B. Volker and S. Hug, EAWAG, Dübendorf, Switzerland).

Results and Discussion

Steady-State Photolysis Detected by Stopped-Flow Technique. Figure 1 presents the results for the decoloration of UB as a function of time. The experimental results as shown in Figure 1 explored the UB decoloration as a function of incident light wavelength from the Xe lamp. The optical arrangement used has been described in the Experimental Section. No dye decoloration was observed after 40 s in irradiated solutions of the dye with air, Fe^{3+} or H_2O_2, using a mercury lamp with λ > 400 nm and λ > 500 nm filters. When Fe^{3+} and H_2O_2 were used together, UB decolorized as

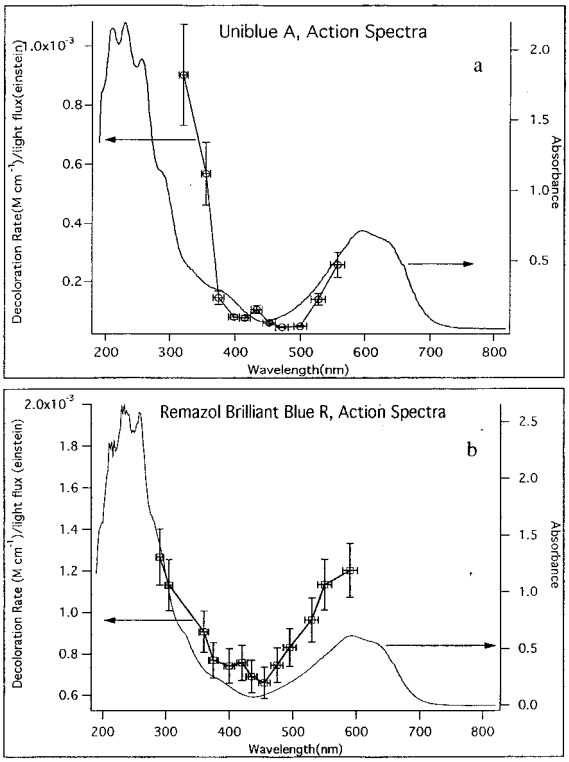

FIGURE 2. (a) Dependence of the rate of Uniblue A decoloration normalized to the photon flux of the incident light vs wavelength of the illumination. The absorbance spectrum of Uniblue A is shown in the same graph to reference the latter results. [Fe^{3+}] = 0.6 mM; [H_2O_2] = 12.5 mM; [Uniblue] = 0.1 mM; pH = 2.4. (b) Dependence of the rate of Remazol Brilliant R decoloration normalized to the photon flux of the incident light vs wavelength of the illumination. The absorbance spectrum of Remazol Brilliant R is shown to reference the latter results. [Fe^{3+}] = 0.6 mM; [H_2O_2] = 12.5 mM; [Remazol] = 0.1 mM; pH = 2.4.

shown in Figure 1 (trace 1). When radiation was applied simultaneously, the rate scale of decoloration increased (traces 2−4). The results in Figure 1 show unambiguously that photosensitized reactions due to the dye in solution are active in Fe^{3+}/H_2O_2-mediated decoloration. The oxidant H_2O_2 absorbs light at λ < 300 nm, and the $FeOH^{2+}$ intermediate (*2*, *4*, *5*) does not absorb light >400 nm at the concentrations used in Figure 1. The results reported in Figure 1 were also observed for the RBB dye where the absorbance deviated only marginally from the values reported for UB. They are, therefore, not shown in Figure 1.

To gain insight into the nature of the chromophore participating in the decoloration of UB as presented in Figure 1, the initial rate of decoloration during the stopped-flow measurements was registered in the photodiode for up to 80 s. The dependence of the initial rate of UB decoloration vs wavelength of the incident light is shown in Figure 1 for UB and RBB dyes. The data was normalized with reference to the water circulating through the system with the following procedure. In Figure 2a, the first point of the action spectrum was obtained by using a filter (1) with a cutoff at λ = 320 nm. Only light with λ > 320 nm goes through and reaches the Uniblue dye. The amount of light with λ > 320 nm was determined by actinometry. The detector beam passes through the sample and the monochromator, set at λ = 590 nm, until it reached the photodiode. The detection beam is monitored at 590 nm independently throughout the experiment and registered. Filter (2) is a second cutoff filter at 580 nm to ensure that any light below the latter wavelength is eliminated, allowing only the detection beam at λ = 590 nm to reach the photodiode.

Next, a filter with a cutoff at 360 nm was set in position (1) in Figure 1a. Again the light passing through and reaching the sample is determined by actinometry and the effect on the monitoring light at λ = 590 nm is monitored and registered. Subsequently, this was repeated for nine points between 380 and 570 nm (action spectrum shown in Figure 2a) employing the same method. This is the basis for the calculation of the quantum efficiency (q.e.) of the incident light defined as the ratio of q.e.(λ) = dye decoloration rate (λ)/incident photon flux (λ). It is readily seen from Figure 2a that the shape of q.e.(λ) depends on wavelength and resembles the absorbance of the UB dye observed in Figure 2a between 400 and 800 nm. This strongly suggests that the excitation of UB enhances the photoassisted Fenton reaction taking place in solution. From Figure 2a, it is seen that although the amount of light varies in the region of 380 to 500 nm the above ratio remains almost the same due to the specific absorption of Uniblue. The decoloration rate is reported by error bars between 320 and 570 nm by the weighted average of the experimental data (1000 points taken at 80 ms interval during 80 s). The quantum yield of decoloration was estimated from the ratio: $\Phi(\lambda)$ = decoloration rate (λ)/adsorbed photon flux (λ). The values $\Phi = 0.23 \pm 0.05$ and $\Phi = 0.29 \pm 0.06$ were found for UB and RBB, respectively, using light with λ > 400 nm. The quantum yield found at 360 nm for UB was $\Phi_{360} = 0.44 \pm 0.07$ and the value for RBB $\Phi_{360} = 0.61 \pm 0.05$. The increase observed in Φ is due to the photodissociation of $Fe(OH)^{2+}$ with ϵ_{366} = 275 M^{-1} cm^{-1}, reaction (1b) (*11*, *12*) and only to a much lesser extent to H_2O_2 with ϵ_{295} = 20 M^{-1} cm^{-1} in reaction (1a).

Laser kinetic spectroscopy of UB and UB−Fe^{3+} complexes in aerated solutions (Figure 3a) shows that the addition of increasing concentrations of Fe^{3+} in UB solutions leads to changes in absorption spectra as shown in traces 1−4. The isosbestic points are seen at λ = 488 nm in Figure 3a for UB and at λ = 682 nm in Figure 3b for RBB. The absorption changes as a function of the concentration of added [Fe^{3+}] obeyed the well-known Benessi−Hildebrand relations (*14*). The application of the Benessi−Hildebrand relationship to calculate the K_{eq} for the Uniblue A−Fe^{3+} complex assumes a complex composition of [Dye:Fe^{3+}] = 1:1. The change in optical density due to the complexation of the Uniblue at 718 nm is seen in Figure 3a showing the variation in absorbance as a function of added Fe^{3+} ion. The linearized Benessi−Hildebrand relation used is shown below in eq 2.

$$\frac{1}{\Delta OD} = \frac{1}{\epsilon_c[Fe^{3+}][dye]K_{eq}} + \frac{1}{\epsilon_c[dye]} \qquad (2)$$

The inverse of the change in the optical density is plotted against the inverse in the Fe^{3+} ion molar concentration, and the intercept over the tangent found for the straight line fit of the experimental points renders the value of K_{eq} in ref *2*. The line shown in the inset of Figure 3a fits the experimental points with a correlation factor >0.998. The equilibria constants K_{eq} for these complexes were found with values $K_{UB} = (2.1 \pm 0.6) \times 10^3$ M^{-1} and $K_{RBB} = (2.2 \pm 0.5) \times 10^3$ M^{-1}.

The transient absorption spectra at different times after the pulse for the UB dye are shown in Figure 4a. The lifetime of the excited-state UB* of $\tau_0 = 1.1 \pm 0.2$ μs is shown in the inset in Figure 4a. These spectra are similar to the transient spectra reported in the literature for 1,4-diaminoanthraquinone, which is the chemical analog of UB (*13*). The transient spectrum with a 100 ns delay can be attributed to the T−T absorption of the dye. In Figure 4a, the UB* molecules almost completely relax to the ground state.

The addition of Fe^{3+} ions to the solution used in Figure 4a reduces the lifetime of UB*, introducing noticeable changes to the former transient absorption spectra reported in Figure 4b. Inset 1 in Figure 4b shows the formation of a longer lived

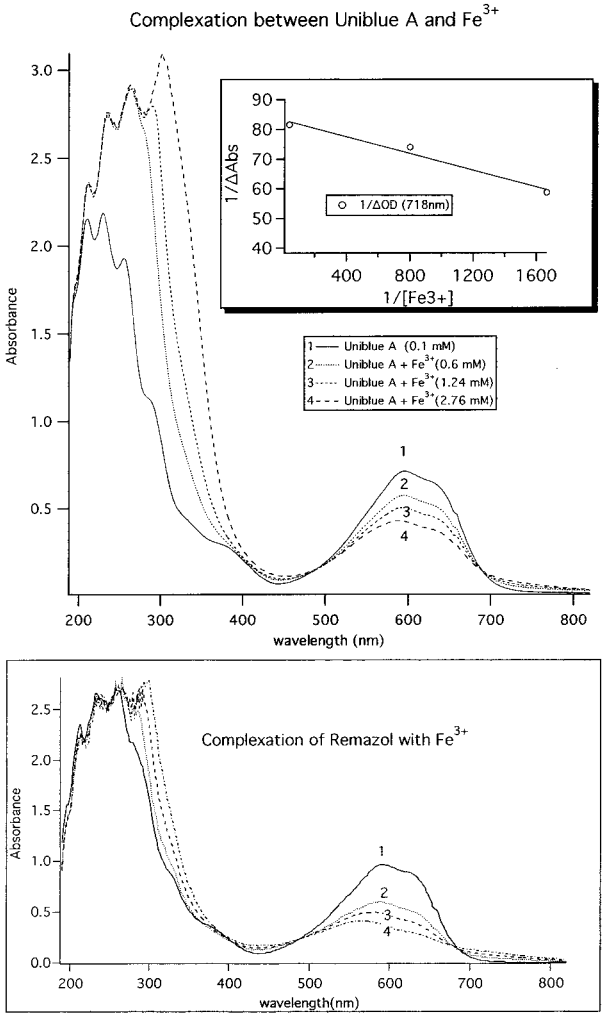

FIGURE 3. (a) Complex formation between Uniblue A and Fe^{3+}. Spectral changes due to the increase of Fe^{3+} concentration are taken in a cell (d = 1 cm). [Uniblue] = 0.1 mM; pH = 2.4. The Benessi−Hildebrand fit is shown in the inset. For other details, see text (1, $[Fe^{3+}]$ = 0.0 mM; 2, $[Fe^{3+}]$ = 0.60 mM; 3, $[Fe^{3+}]$ = 1.24 mM; 4, $[Fe^{3+}]$ = 2.76 mM). (b) Complex formation between Remazol Brilliant R and Fe^{3+}. Spectral changes due to the increase of Fe^{3+} concentration are taken in a cell (d = 1 cm). [Remazol] = 0.16 mM; pH = 2.3 (1, $[Fe^{3+}]$ = 0.0 mM; 2, $[Fe^{3+}]$ = 1.0 mM; 3, $[Fe^{3+}]$ = 5.0 mM; 4, $[Fe^{3+}]$ = 10 mM).

photoproduct by the plateau formation up to 3 μs. A plot showing the reciprocal of the lifetime of UB* as a function of added $[Fe^{3+}]$ is shown next in inset 2 (Figure 4b). The quenching rate constant found for the UB* by the Fe ion was seen in this case to be $k_q = (1.2 \pm 0.3) \times 10^9$ (M s)$^{-1}$, close to the diffusion controlled value.

This quenching occurs because of electron transfer from UB* to Fe^{3+}. The long-lived product in Figure 4b can be attributed to the cation radical $UB^{+\bullet}$. Electron transfer between UB* and Fe^{3+} is thermodynamically favorable if we consider the following: (a) $E_{1/2}(UB/UB^+) = 1.038$ V vs NHE, (b) $E_{1/2}(Fe^{2+}/Fe^{3+}) = 0.77$ V vs NHE, and (c) assuming that the triplet energy level of UB(ET) resembles the *ET* of 1,4-diaminoanthraquinone of 1.27 eV, then $\Delta G = E_{1/2}(UB/UB^+) - E_{1/2}(Fe^{2+}/Fe^{3+}) - ET = 1.038 - 0.77 - 1.27 = -1$ eV. The most likely result of the electron transfer is Fe^{2+} (*4*−*6*). Control experiments with Fe^{3+}(aq) are not included in this study because at the pH and concentrations worked and the wavelength of light used no Fe^{3+} aquo-complexes were observed that could overlap with the Fe^{3+} dye transient spectrum.

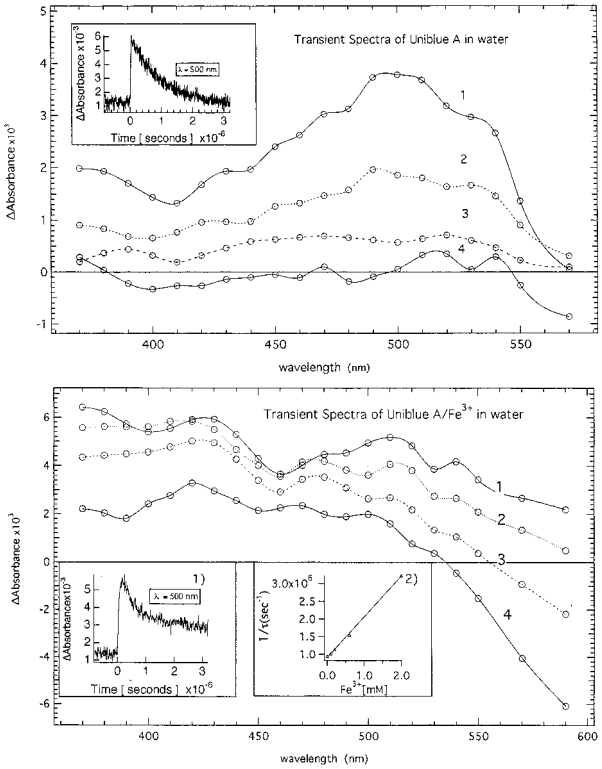

FIGURE 4. (a) Transient absorption spectra of Uniblue A under laser excitation λ_{ex} = 347 nm. pH = 2.4. Trace 1, delay of the signal after the laser pulse: 1.0×10^{-7} s; trace 2, delay of the signal after the laser pulse: 8.0×10^{-7} s; trace 3, delay of the signal after the laser pulse: 1.6×10^{-6} s; trace 4, delay of the signal after the laser pulse 6.4×10^{-6} s. (b) Transient absorption spectra of Uniblue A in the presence of Fe^{3+} under laser excitation λ_{ex} = 347 nm; $[Fe^{3+}]$ = 0.3 mM; pH = 2.4. Trace 1, delay of the signal after the laser pulse 1.0×10^{-7} s; trace 2, delay of the signal after the laser pulse 4.0×10^{-7} s; trace 3, delay of the signal after the laser pulse 1.6×10^{-6} s; trace 4, delay of the signal after the laser pulse 6.4×10^{-6} s; inset, plot of the reciprocal lifetime of the excited dye vs Fe^{3+} concentration.

To explain the experimental results observed in the presence of increasing quencher concentration, a redox photodissociation is suggested of the complex $[D\cdots Fe^{3+}] \xrightarrow{h\nu} D^{\bullet+} + Fe^{2+}$ (*2*, *4*). At Fe^{3+} concentrations of 1 mM, most of the dye molecules would be complexed by the excess Fe^{3+} in solution. The results in Figure 4b suggest that the photooxidation of UB* (or RBB*) proceeds through bimolecular quenching by Fe^{3+} ions or through the photodissociation of the $[D\cdots Fe^{3+}]$ complex. In separate experiments, no substantial quenching of excited UB* (or RBB*) by air or H_2O_2 was observed. The transient decay showed about the same amplitude and lifetime in solutions with one atmosphere of Ar or air. The addition of H_2O_2 (100 mM) did not lead to changes in the transient decay as compared to the case of no oxidant addition in solution. In agreement with the laser flash photolysis experiments, the photoreduction of Fe^{3+} by the dye detected by stopped-flow could be ascribed to: (1) the Fe^{3+} reduction during photolysis of the $[UB\cdots Fe^{3+}]$ complex, and (2) Fe^{3+} reduction during the bimolecular quenching of UB* molecules. In case (1), the rate of the reaction of Fe^{3+} photoreduction (to Fe^{2+}) can be written under steady-state illumination:

$$D + Fe^{3+} = [D\cdots Fe^{3+}] \xrightarrow{h\nu} D^{\bullet+} + Fe^{2+} \qquad (3)$$

$$\frac{d[Fe^{2+}]}{dt} = \frac{K_{eq}\cdot[D]_0\cdot[Fe^{3+}]\cdot I\cdot\phi_1\cdot\alpha_1}{1 + K_{eq}\cdot[Fe^{3+}]} = k_{eff}^{(1)}\cdot[D]_0\cdot[Fe^{3+}] \quad (4)$$

where $[D]_0$ (see Addendum I for details of eq 4) is the dye concentration in the bonded and nonbonded forms, ϕ_1 is the yield of the $[D\cdots Fe^{3+}]$ complex photodissociation, and α_1 is the complex absorption coefficient.

$$k_{eff}^{(1)} = \frac{K_{eq} I \phi_1 \alpha_1}{1 + K_{eq}[Fe^{3+}]} \quad (5)$$

In case (2), the rate of the reaction (3) under steady-state illumination can be written for the quasistationary state concentration of the excited dye molecules D*

$$D \xrightarrow{h\nu} D^* + Fe^{3+} \xrightarrow{k_q} [D^{\bullet+} \bullet\bullet\bullet Fe^{2+}] \begin{matrix} \rightarrow D^{\bullet+} + Fe^{2+} \\ \rightarrow D + Fe^{3+} \end{matrix} \quad (6)$$

$$\frac{d[Fe^{2+}]}{dt} = \phi_2 \bullet k_q \bullet [D^*] \bullet [Fe^{3+}] = \phi_2 \bullet \frac{I \bullet \alpha_2 \bullet k_q}{k_q \bullet [Fe^{3+}] + 1/\tau_0} \bullet [D] \bullet [Fe^{3+}] = k_{eff}^{(2)} \bullet [D]_0 \bullet [Fe^{3+}] \quad (7)$$

where ϕ_2 (see Addendum II for details of eq 7) is the yield of radicals escaping from cage recombination during the quenching of D* by Fe^{3+}, I is the light intensity, α_2 is the absorption coefficient, τ_0 is the lifetime of the excited dye, and [D] is the concentration of the noncomplexed dye in solution. It follows:

$$k_{eff}^{(2)} = \frac{I\alpha_2 k_q}{k_q[Fe^{3+}] + 1/\tau_0} \frac{1}{1 + K_{eq}[Fe^{3+}]} \quad (8)$$

The rate of Fe^{3+} photoreduction to Fe^{2+}, proceeds involving the concentration of dye molecules [D] as $k_{eff}[D][Fe^{3+}]$ as shown in eq 8. The decoloration of UB at each Fe^{3+} and H_2O_2 concentration and also as a function of light intensities were followed by stopped-flow. This allowed insight into the decoloration taking place and the ability to model this process.

Modeling. The mathematical modeling is based on the chain radical mechanism of the Fenton process as shown in Scheme 1. The parameter k_{eff} is used during the fitting of the decoloration kinetics observed by the stopped-flow technique at different concentrations of Fe^{3+}, H_2O_2, and light intensities.

SCHEME 1

Chain initiation		
$D + Fe^{3+} \xrightarrow{+h\nu} D^{\bullet+} + Fe^{2+}$	k_{eff} = adjustable parameter	(9)
$FeOOH^{2+} \rightarrow Fe^{2+} + HO_2$	$k_{10} = 2 \times 10^{-3}\ s^{-1}$	(10)
$FeOOH^{2+} + FeOH^{2+} \rightarrow 2Fe^{2+} + O_2 + H_2O$	$k_{11} = 5\ (M\ s)^{-1}$	(11)
Chain propagation		
$Fe^{2+} + H_2O_2 \rightarrow Fe^{3+} + {}^{\bullet}OH + OH^-$	$k_{12} = 53\ (M\ s)^{-1}$	(12)
${}^{\bullet}OH + H_2O_2 \rightarrow HO_2^{\bullet} + H_2O$	$k_{13} = 3.0 \times 10^7\ (M\ s)^{-1}$	(13)
$O_2^{\bullet-} + Fe^{3+} \rightarrow Fe^{2+} + O_2^{\bullet}$	$k_{14} = 1 \times 10^9\ (M\ s)^{-1}$	(14)
Chain termination		
$Fe^{2+} + HO_2^{\bullet} \rightarrow Fe^{3+} + HO_2^-$	$k_{15} = 8 \times 10^5\ (M\ s)^{-1}$	(15)
$Fe^{2+} + {}^{\bullet}OH \rightarrow Fe^{3+} + OH^-$	$k_{16} = 4 \times 10^8\ (M\ s)^{-1}$	(16)
$HO_2^{\bullet} + HO_2^{\bullet} \rightarrow H_2O_2 + O_2$	$k_{17} = 1.8 \times 10^6\ (M\ s)^{-1}$	(17)
Acid-base equilibria		
$H_2O_2 = H^+ + HO_2$	$K_{18} = 2.63 \times 10^{-12}\ M$	(18)
$HO_2^{\bullet} = H^+ + O_2^{\bullet-}$	$K_{19} = 3.55 \times 10^{-6}\ M$	(19)
$Fe^{3+} + H_2O = FeOH^{2+} + H^+$	$K_{20} = 1.8 \times 10^{-3}\ M$	(20)
$Fe^{3+} + H_2O_2 = FeOOH^{2+} + H^+$	$K_{21} = 2.0 \times 10^{-3}\ M$	(21)

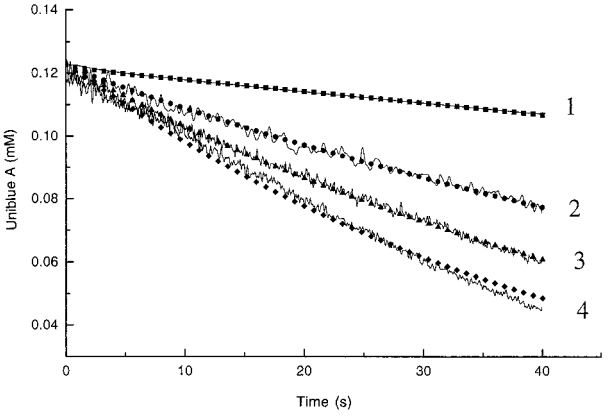

FIGURE 5. Comparison of experimental traces of the dye concentrations obtained by stopped-flow at the different light power densities and model curves (symbols) calculated by Scheme 1. k_{eff} values are shown in this figure. $[Fe^{3+}] = 0.375$ mM; $[H_2O_2] = 50$ mM; [Uniblue A] = 0.1 mM; pH = 2.4 (1, light intensity = 0.15 W/m^2; 2, light intensity = 0.29 W/m^2; 3, light intensity = 0.50 W/m^2; 4, light intensity = 0.85 W/m^2).

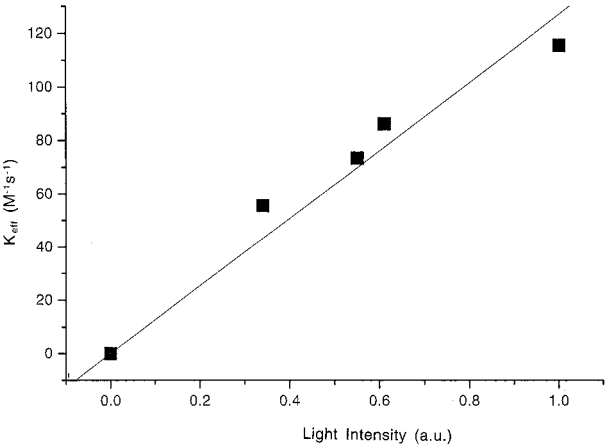

FIGURE 6. Dye is Uniblue A. Dependence of k_{eff} on intensity during the decoloration of Uniblue A. Light intensity is in arbitrary units. Incident light with 0.85 W/cm^2 corresponds to one unit.

This parameter k_{eff} is a function of light intensity, Fe^{3+} concentration, and H_2O_2 concentration, and the plots of k_{eff} are different for the different Fe^{3+} and H_2O_2 concentrations and light intensities used. The correlation between $1/k_{eff}$ in Figures 6 and 8 allow one to draw conclusions about the mechanism intervening in Fe^{3+} photoreduction to Fe^{2+}.

In Scheme 1, the rate constant values were taken from refs *2*, *4*−*6*, and *15*. The rate constants for radical reactions were taken from the pulse radiolysis data for reactions of the $HO^{\bullet}$ radical with organic molecules in the absence of iron species. This approach restricts the ambiguity in the fitting of the experimental data compared to the multivariable approach as reported elsewhere (*16*) since it adjusts the value of only one parameter, k_{eff}.

In Scheme 1, the Fe^{3+}/H_2O_2-mediated oxidation of aromatics leads to the formation of adducts with $HO^{\bullet}$ radicals (eq 7). Reactions of these radicals with O_2 also contribute to the final product formation. Rate constants of reactions 17 and 18 were estimated from dark, stopped-flow experiments used in the fitting of the experiments under light irradiation. Figure 5 presents the experimental traces and model points found for different intensities at constant Fe^{3+} and H_2O_2 concentrations, taking the best fit possible when varying the values of k_{eff}.

Figure 6 shows the linear dependence between the k_{eff} value and the intensity of the light irradiation used. The

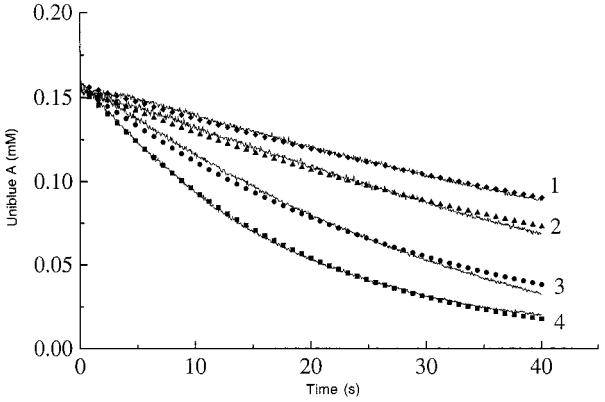

FIGURE 7. Comparison of experimental dye concentrations obtained by stopped-flow at different [Fe^{3+}] concentrations and the curves predicted by the modeling used (symbols). [H_2O_2] = 12.5 mM; [Uniblue A] = 0.1 mM; pH = 2.4. Trace 1, [Fe^{3+}] = 0.047 mM; trace 2, [Fe^{3+}] = 0.094 mM; trace 3, [Fe^{3+}] = 0.375 mM; trace 4, [Fe^{3+}] = 0.750 mM.

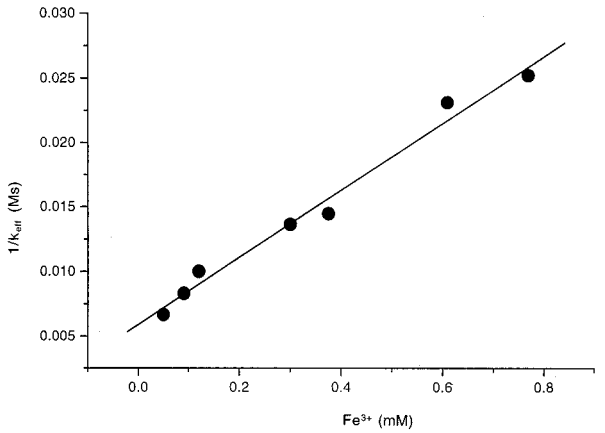

FIGURE 8. Dye is Uniblue A. Dependence of the reciprocal k_{eff} value on [Fe^{3+}] concentration. Light intensity is 1.2 W/cm². [H_2O_2] = 12.5 mM; [Uniblue A] = 0.1 mM; pH = 2.4.

observed linear dependence was predicted by way of the rates in eq 5 or 8. When the H_2O_2 concentration was varied from 12 to 100 mM at constant UB and Fe^{3+} concentrations, no changes of k_{eff} were observed within an error limit of 8%. This result is in agreement with eqs 5−8.

Figure 7 shows the kinetic traces obtained by stopped-flow techniques as a function of the iron concentration used in each trace. In the case of mechanism (1) $D + Fe^{3+} \rightarrow [D\cdots Fe^{3+}] \xrightarrow{h\nu} D^{\bullet+} + Fe^{2+}$ as mentioned in eq 3, the Fe^{2+} in solution would be produced due to the photodissociation of the complex [D···Fe^{3+}].

From the evidence presented until now, the Fe^{3+} photoreduction to Fe^{2+} seems to follow several ways. The first model (a) may proceed through the photoreduction of Fe^{3+} to Fe^{2+} through the photodissociation of the complex (D···Fe^{3+}). In this case, k_{eff}^{1} should fit the experimental data. A second model is possible for this reaction where (b) the photoreduction of Fe^{3+} to Fe^{2+} occurs through reaction of D* and Fe^{3+}. In the case of mechanism (b), the formation of Fe^{2+} is suggested to involve a bimolecular quenching reaction (eq 6). In the latter case, k_{eff}^{2} should fit the experimental data.

Figure 8 shows the fit of the experimental points of $(k_{eff}^{1})^{-1}$ plotted vs the Fe^{3+} concentration after eq 5. Statistical analysis of the dependence of (k_{eff}^{-1}) vs [Fe^{3+}] gives a linear fit of the form $A + Bx$ with $A = (5.91 \pm 0.62) \times 10^{-3}$ M s, $B = 26 \pm 1.5$ s, and R (correlation factor) = 0.992. For the case of the model (b), a plot of $(k_{eff}^{2})^{-1}$ vs Fe^{3+} concentration after eq 8, a quadratic polynomial, also renders a linear plot not shown in Figure 8 because it was very close to the previous one. The quadratic polynomial fit of the form $A + Bx + Cx^2$ with $A = (5.85 \pm 1.0) \times 10^{-3}$, $B = 26.5 \pm 0.7$ s, $C = 2.6 \pm 0.8 \times 10^{-4}$ s/M, and $R = 0.983$. From the correlation coefficient of the linear dependence and the magnitude of C, it can be concluded that the formation of Fe^{2+} occurs predominantly through the mechanism (a) involving photodissociation of (D···Fe^{3+}) following a linear and not a quadratic expression.

From eq 5, the ratio B/A in the linear dependence between $1/k_{eff}$ and Fe^{3+} is equal to the equilibrium constant $K_{eq} = (4.18 \pm 1.8) \times 10^3$ M^{-1} for the complex formation between D and Fe^{3+}. This value is close to the value of $K_{eq} = (2.1 \pm 0.6) \times 10^3$ M^{-1} measured independently by spectrophotometry and calculated by the Benessi-Hildebrand relations previously mentioned. The latter consideration provides additional evidence for the validity of Scheme 1.

In conclusion, the decoloration kinetics of photoassisted Fe^{3+}/H_2O_2 reactions of Remazol Brilliant Blue R (RBB) and Uniblue A (UB) have been modeled and were observed to be in good agreement with the sequence proposed for the individual reactions. The quenching of RBB* and UB* is due mainly to the interaction with Fe^{3+} by electron-transfer reactions as seen by laser photolysis and stopped-flow techniques. Laser flash photolysis suggested bimolecular quenching of the excited dye $Fe^{3+} + D \xrightarrow{+h\nu} D^* + Fe^{3+} \xrightarrow[k_q = 1.2 \times 10^9\ (M\ s)^{-1}]{} D^{\bullet+} + Fe^{2+}$ and photodissociation of the complex $D + Fe^{3+} \overset{Keq}{\leftrightarrow} [D\cdots Fe^{3+}] \xrightarrow{+h\nu} D^{\bullet+} + Fe^{2+}$ with the values $K_{eq} = 2.1 \times 10^3$ M^{-1} and 2.3×10^3 M^{-1} for Uniblue A for Remazol, respectively. The dependency of k_{eff} on light intensity and [Fe^{3+}] indicated that the enhancement of the decoloration in the Fe^{3+}/H_2O_2-mediated reactions was mainly due to $D + Fe^{3+} \rightarrow [D\cdots Fe^{3+}] \xrightarrow{+h\nu} D^{\bullet+} + Fe^{2+}$. The quenching rate constant between D* and Fe^{3+} ion was found to be $(1.2 \pm 0.3) \times 10^9$ $(M\ s)^{-1}$, a value close to diffusion controlled reactions. The quenching was due to the electron transfer from D* to Fe^{3+}. The system used removes color in seconds to minutes depending on the dye concentration from strongly colored solutions under light irradiation. Moreover, since visible light was used, it shows that solar energy is sufficient to activate these kinds of processes.

Acknowledgments

This work was supported by the Commission of the European Communities Environmental Program (Grant No. ENV-CT-0064, OFES).

Addendum 1

For eq 4:
from

$$D + Fe^{3+} = [D\cdots Fe^{3+}] \xrightarrow{h\nu} D^{\bullet+} + Fe^{2+}$$

with

$$K_{eq} = \frac{[D\cdots Fe]^{3+}}{[D][Fe^{3+}]}$$

The rate of Fe^{2+}

$$\frac{d}{dt}[Fe^{2+}] = \alpha_1 \Phi_1 I [D\cdots Fe]^{3+}$$

where Φ_1 = quantum yield, I = light intensity, and α_1 = absorption coefficient and considering mass balance

$$[D_0] = [D] + [D\cdots Fe]^{3+} \Rightarrow [D_0] = [D] + K_{eq}[D][Fe^{3+}]$$

Then

$$[D\cdots Fe]^{3+} = \frac{K_{eq}[D][Fe^{3+}]}{1 + K_{eq}[Fe^{3+}]}$$

$$\frac{d}{dt}[Fe^{2+}] = \frac{\alpha_1 \Phi_1 I K_{eq}[D][Fe^{3+}]}{1 + K_{eq}[Fe^{3+}]} = k^1_{eff}[D_0][Fe^{3+}] \quad \text{(eq 4)}$$

Addendum II

For eq 7:

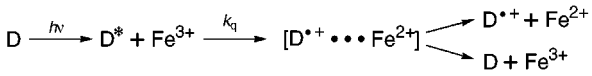

The formation of Fe^{2+}

$$\frac{d}{dt}[Fe^{2+}] = \Phi_2 k_q [D^*][Fe^{3+}]$$

and

$$\frac{d}{dt}[D^*] = I\alpha_2[D]$$

$$\frac{d}{dt}[D^*] = \left\{k_q[Fe^{3+}] + \frac{1}{\tau_0}\right\}[D^*] \qquad \text{Stern–Volmer}$$

$$[D^*] = \frac{\Phi_2 k_q I[D][Fe^{3+}]}{k_q[Fe^{3+}] + \frac{1}{\tau_0}}$$

and using the mass balance from Addendum I

$$\frac{d}{dt}[Fe^{2+}] = \frac{\Phi_2 k_q I[D][Fe^{3+}]}{\left\{k_q[Fe^{3+}] + \frac{1}{\tau_0}\right\}\{K_{eq}[Fe^{3+}] + 1\}} = k^2_{eff}[D_0][Fe^{3+}] \quad \text{(eq 7)}$$

Glossary

ΔOD	change in optical density
ϵ_c	molar absorption coefficient of the complex
$[Fe^{3+}]$	initial concentration of Fe in the solution
K_{eq}	equilibrium constant

Literature Cited

(1) Ollis, D. F., Al-Ekabi, H., Eds. *Photocatalytic Purification and Treatment of Water and Air*; Elsevier: Amsterdam, 1993.

(2) (a) Sun, Y.; Pignatello, J. *J. Agric. Food Chem*. **1992**, *40*, 322. (b) Pignatello, J. *Environ. Sci. Technol*. **1992**, *26*, 944. (c) Safarzadeh-Amiri, A.; Bolton, J. R.; Carter, S. R. *J. Adv. Oxid. Technol*. **1996**, *1*, 18. (d) Oliveiros, E.; Legrini, O.; Braun, A. M.; Hohl, M.; Muller, T. *Water Sci. Technol*. **1997**, *35*, 223. (e) Nadtochenko, V.; Kiwi, J. *J. Chem. Soc., Faraday Trans*. **1996**, *93*, 2373. (f) Halmann, M. *Photodegradation of Water Pollutants*; CRC Press: Boca Raton, FL, 1996.

(3) (a) Ruppert, G.; Bauer, R.; Heisler, G. *J. Photochem. Photobiol., A: Chem*. **1993**, *73*, 75.

(4) Nadtochenko, V.; Kiwi, J. *Environ. Sci. Technol*. **1998**, in press.

(5) Nadtochenko, V.; Kiwi, J. *J. Chem. Soc., Perkin Trans. 2* **1998**, 1303.

(6) Nadtochenko, V.; Kiwi, J. *J. Photochem. Photobiol., A: Chem*. **1996**, *99*, 145.

(7) Walling, C. *Acc. Chem. Res*. **1975**, *8*, 125.

(8) Bossman, S.; Oliveros, E.; Gob, S.; Siegwart, S.; Dahlen, E.; Payawan, L.; Straub, M.; Wörner, M.; Braun, A. *J. Chem. Phys. A* **1998**, *102*, 5542.

(9) Faust, C.; Hoigné, J. *J. Atm. Environ*. **1990**, *24*, 79.

(10) Huy, A.; Bolton, J. Abstracts ACS, Division of Environmental Chemistry, Chicago, IL, 1995; p 555.

(11) Zepp, R.; Faust, B.; Hoigné, J. *Environ. Sci. Technol*. **1992**, *26*, 13.

(12) Knight, R.; Silva, J. *J. Inorg. Nucl. Chem*. **1975**, *37*, 779.

(13) Palit, K. D.; Pal, H.; Mukherjee, T.; Mittal, P. *J. Photochem. Photobiol., A: Chem*. **1990**, *52*, 375.

(14) Bennessi, H.; Hildebrand, H. *J. Am. Chem. Soc*. **1949**, *71*, 2703.

(15) Sychev, Ya.; Isak, G. *Russ. Chem. Rev*. **1995**, *64*, 1105.

(16) Okino, M. S.; Mavrovouniotis, M. L. *Chem. Rev*. **1998**, *98*, 391.

Received for review September 25, 1998. Revised manuscript received April 27, 1999. Accepted June 17, 1999.

ES980995+